ACS Catalysis

Research Article

pubs.acs.org/acscatalysis

Efficient and Mild Carbon Dioxide Hydrogenation to Formate Catalyzed by Fe(II) Hydrido Carbonyl Complexes Bearing 2,6-(Diaminopyridyl)diphosphine Pincer Ligands

Federica Bertini,[†] Nikolaus Gorgas,[‡] Berthold Stöger,[§] Maurizio Peruzzini,[†] Luis F. Veiros,[∥] Karl Kirchner,*[,‡] and Luca Gonsalvi*[,†]

[†]Consiglio Nazionale delle Ricerche (CNR), Istituto di Chimica dei Composti Organometallici (ICCOM), Via Madonna del Piano 10, 50019 Sesto Fiorentino (Firenze), Italy

[‡]Institute of Applied Synthetic Chemistry and [§]Institute of Chemical Technologies and Analytics, Vienna University of Technology, Getreidemarkt 9/163-AC, A-1060 Wien, Austria

[§]Institute of Chemical Technologies and Analytics, Vienna University of Technology, Getreidemarkt 9/163-AC, A-1060 Wien, Austria

[∥]Centro de Química Estrutural, Instituto Superior Técnico, Universidade de Lisboa, Av. Rovisco Pais No. 1, 1049-001 Lisboa, Portugal

Supporting Information

ABSTRACT: Fe(II) hydrido carbonyl complexes supported by PNP pincer ligands based on the 2,6-diaminopyridine scaffold were found to promote the catalytic hydrogenation of CO_2 and $NaHCO_3$ to formate in protic solvents in the presence of bases, reaching quantitative yields and high TONs under mild reaction conditions, with pressures as low as 8.5 bar and temperatures as low as 25 °C. NMR and DFT studies highlighted the role of dihydrido and hydrido formate complexes in catalysis.

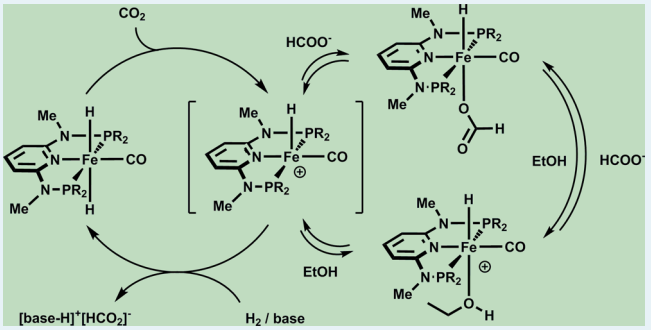

KEYWORDS: *CO_2 hydrogenation, iron pincer complexes, homogeneous catalysis, mechanistic studies, DFT calculations*

INTRODUCTION

The use of CO_2 as a C1 source is a matter of great interest due to its high abundance, availability, and low cost. In particular, its reduction to HCOOH or derivatives has attracted significant attention in recent years, since it holds the potential for reversible hydrogen storage.[1] The reduction of $NaHCO_3$ is also of interest, as CO_2 can be easily trapped in basic solutions and reversible hydrogen storage cycles based on bicarbonate and formate have been proposed.[2] The most efficient catalysts for CO_2 hydrogenation are typically based on expensive noble metals such as ruthenium and iridium.[3] In the quest for cheaper alternatives, the preparation of well-defined earth-abundant metal catalysts of comparable activity is highly desirable and important progress has been made recently.[4] Efficient iron-based catalysts supported by tetraphosphine ligands have been reported by Beller[4a,b] and some of us,[4c] whereas Milstein reported that the iron pincer complex [Fe(PNP)$(H)_2$(CO)] (PNP = 2,6-bis(di-*tert*-butylphosphinomethyl)pyridine) catalyzes CO_2 hydrogenation at low pressure.[4d] More recently, Hazari and co-workers achieved impressive catalytic activities in Fe-catalyzed CO_2 hydrogenation, reaching turnover numbers (TONs) up to 79600 using iron PNP pincer complexes in the presence of Lewis acid (LA) cocatalysts.[4e] In recent years, some of us developed a new class of PNP pincer complexes based on the 2,6-diaminopyridine scaffold where the PR_2 moieties of the PNP ligand are connected to the pyridine ring via NH, N-alkyl, or N-aryl spacers.[5] Among these, the iron hydrido carbonyl complexes [Fe(PNP^H-*i*Pr)(H)(CO)(Br)] (**1**) and [Fe(PNP^{Me}-*i*Pr)(H)(CO)(Br)] (**2**), shown in Scheme 1, were shown to be active catalysts for hydrogenation reactions.[5c] Mechanistic studies showed that the N−H spacer of the PNP ligand in **1** can work as a bifunctional catalyst promoting metal−ligand cooperation,[5c,d] while the N−Me spacer in complex **2** prevents

Scheme 1. Fe-PNP Pincer Complexes 1 and 2

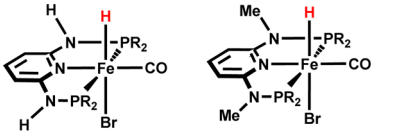

Received: February 10, 2016
Revised: March 26, 2016

DOI: 10.1021/acscatal.6b00416
ACS Catal. XXXX, XXX, XXX−XXX

such a possibility. In addition, the presence of a labile bromide and strongly σ donating H and CO ligands could give an ideal donor set suitable for catalytic CO_2 hydrogenation.[4d] Thus, we investigated the activities of these complexes for CO_2 and $NaHCO_3$ hydrogenation reactions.

RESULTS AND DISCUSSION

Catalytic Studies. Initially, the catalytic activities of **1** and **2** in $NaHCO_3$ hydrogenation were tested in different solvents using 0.05 mol % of catalyst at 80 °C, 90 bar of H_2, and 24 h (Table S1 in the Supporting Information). The best results were obtained in H_2O/THF (4/1) mixtures which ensure good solubility of both catalysts and substrate, reaching 98% formate yield and TON = 1964 for **1** and 52% formate yield and TON = 1036 for **2**, respectively. In MeOH, TONs and yields decrease by ca. 50% with both catalysts, whereas the reaction does not proceed in neat THF, indicating the need for a protic solvent. In all cases, **1** performed better than **2** under analogous conditions (see the Supporting Information for details). On the basis of the solvent screening results, the hydrogenation of $NaHCO_3$ in H_2O/THF was then studied with **1** under different conditions of temperature, pressure, and catalyst loading (Table 1). In the presence of only 0.005 mol % of **1**, TONs up to 4560 could be achieved at 80 °C and 90 bar of H_2 after 24 h (entry 2). Either higher or lower temperatures resulted in lower turnover numbers (entries 3 and 4). It is worth noting that the reaction proceeds *even at room temperature*, giving TON = 188 after 72 h (entry 5). Reducing the H_2 pressure resulted in a drop of TONs (entries 6 and 7), yet at higher catalyst loadings (0.1 mol %) sodium formate was obtained (14% yield) with a TON of 140 at only 8.5 bar of H_2 (Milstein's conditions)[4d] after 16 h (entry 8).

Table 1. Hydrogenation of $NaHCO_3$ to $NaHCO_2$ with 1 at Different Catalyst Loadings, Temperatures, and Pressures[a]

entry[a]	amt of cat. **1** (mol %)	T (°C)	P (bar)	TON[b]	t (h)	yield[c] (%)
1	0.05	80	90	1964	24	98
2	0.005	80	90	4560	24	23
3	0.005	100	90	400	24	2
4	0.005	60	90	2360	24	12
5	0.05	25	90	188	72	9
6	0.005	80	60	640	24	3
7	0.005	80	30	80	24	<1
8	0.1	80	8.5	140	16	14

[a]General reaction conditions: 20 mmol of $NaHCO_3$, 0.01−0.001 mmol of catalyst, 25 mL of H_2O/THF 4/1, 80 °C, 90 bar, 24 h. [b]TON = (mmol of formate)/(mmol of catalyst). [c]Yields calculated from the integration of ^{1}H NMR signals due to $NaHCO_2$, using DMF as internal standard.

Next, the hydrogenation of CO_2 to formate in H_2O/THF (4/1) in the presence of **1** and NaOH as base was studied (Table 2), reaching TONs up to 1220 with nearly quantitative yield under the optimized conditions (catalyst/NaOH = 1/1250, CO_2/H_2 = 40/40 bar, 80 °C, 21 h).

Higher NaOH/catalyst ratios gave worse results regardless of concentration (Table 2, entries 2−4). We then tested the hydrogenation of CO_2 with **1** in EtOH in the presence of different amine bases. Quite surprisingly, formate was not formed using either DBU (1,8-diazabicyclo[5.4.0]undec-7-ene) or DMOA (*N*,*N*-dimethyloctylamine), whereas in the presence of NEt_3 formate was obtained only in low yields (entries 5−7). The observation that complex **1** fails to catalyze the hydrogenation of CO_2 in EtOH in the presence of amine bases such as DBU and DMOA may be attributed to the fact that EtOH appears to prevent the formation of dihydrides,[5c] which are expected to be the catalytically active species in this reaction. No reaction occurred in EtOH in the absence of base (entry 8) or in THF with DBU as base due to catalyst decomposition (entry 9).

Table 2. Hydrogenation of CO_2 to Formate with 1 using Different Solvents and Bases[a]

entry	amt of cat. **1** (mol %)	base	solvent	TON[e]	yield[f] (%)
1	0.08	NaOH	H_2O/THF	1220	98
2[b]	0.04	NaOH	H_2O/THF	608	24
3[c]	0.008	NaOH	H_2O/THF	120	1
4[d]	0.04	NaOH	H_2O/THF	656	26
5	0.08	DBU	EtOH	0	0
6	0.08	DMOA	EtOH	0	0
7	0.08	NEt_3	EtOH	288	23
8	0.08		EtOH	0	0
9	0.08	DBU	THF	0	0

[a]General reaction conditions: 12.5 mmol of base, 0.01 mmol of catalyst, 25.0 mL of solvent, 80 °C, 80 bar total pressure, 21 h. [b]25.0 mmol of base. [c]0.001 mmol of catalyst. [d]0.005 mmol of catalyst. [e]TON = (mmol of formate)/(mmol of catalyst). [f]Yields calculated from the integration of ^{1}H NMR signals due to $NaHCO_2$, using DMF as internal standard.

A complete screening of the effects of catalyst concentration, nature of base, solvent, and temperature for CO_2 hydrogenation in the presence of **2** was then carried out (Table 3).

As for $NaHCO_3$ hydrogenation, catalyst **2** showed poorer performance in comparison to **1** in the hydrogenation of CO_2 in H_2O/THF (4/1) in the presence of NaOH (Table 3, entries 1 and 2, vs Table 2, entries 1 and 2). Among the alcohols, reactions in EtOH gave activity comparable to that observed in H_2O/THF (entry 4), whereas worse performance was achieved in MeOH (Table 3, entry 3). On the basis of the solvent screening results, amine screening was then studied for CO_2 hydrogenation with **2** in EtOH. To our delight, using DBU as base gave nearly quantitative formate yield (>90%) with a TON of 1153 at 80 °C under 80 bar total pressure (entry 5). Using either DMOA or NEt_3 instead of DBU resulted in lower TONs (entries 6 and 7), and no reaction occurred in the absence of base (entry 8) or with DBU in THF (entry 9) under otherwise analogous conditions.

The potential of catalyst **2** was then further explored under milder reaction conditions. At first, the effect of lower total pressure was determined. In the presence of 0.1 mol % of **2** a TON of 480 was reached after 21 h at 80 °C under only 8.5 bar of H_2/CO_2 (1/1) (Table 3, entry 10), an activity comparable to that of other known iron pincer catalysts.[4d,f] Then, temperature effects were studied. At 25 °C, catalyst **2** manifested a remarkable catalytic activity, affording sodium formate in high yields[6] with a TON of 856 after 21 h and of 1032 after 72 h under 80 bar initial pressure (entries 11 and 12) in the presence of 0.1 mol % catalyst. To the best of our knowledge, these are *the highest TONs obtained for Fe-catalyzed CO_2 hydrogenation at room temperature* to date.

Finally, the effect of catalyst loading was studied. At lower catalyst loading (0.01 mol %) sodium formate was still obtained in excellent yield (98%) with a TON of 9840 after 21 h at 80

DOI: 10.1021/acscatal.6b00416
ACS Catal. XXXX, XXX, XXX−XXX

Table 3. Hydrogenation of CO_2 to Formate with 2 using Different Solvents and Bases[a]

entry	amt of cat. 2 (mol %)	base	solvent	T (°C)	TON[i]	yield[j] (%)
1	0.08	NaOH	H_2O/THF	80	680	54
2[b]	0.04	NaOH	H_2O/THF	80	372	15
3	0.08	NaOH	MeOH	80	220	18
4	0.08	NaOH	EtOH	80	654	53
5	0.08	DBU	EtOH	80	1153	92
6	0.08	DMOA	EtOH	80	452	36
7	0.08	NEt_3	EtOH	80	686	55
8	0.08		EtOH	80	0	0
9	0.08	DBU	THF	80	0	0
10[c,d]	0.1	DBU	EtOH	80	480	48
11[c]	0.1	DBU	EtOH	25	856	86
12[c,e]	0.1	DBU	EtOH	25	1032	103
13[c,f]	0.01	DBU	EtOH	80	9840	98
14	0.01	DBU	EtOH	25	465	5
15	0.005	DBU	EtOH	80	10275	21
16[c,g]	0.001	DBU	EtOH	80	5000	5
17[c,f,h]	0.01	DBU	EtOH	80	620	6
18[a]		DBU	EtOH	80	0	0
19[k]	0.08	DBU	EtOH	80	1163	93

[a]General reaction conditions: 12.5 mmol of base, 0.01 mmol of catalyst, 25.0 mL of solvent, 21 h. [b]25.0 mmol of base. [c]10.0 mmol of base. [d]8.5 bar (CO_2/H_2 = 1/1) total pressure. [e]72 h. [f]0.001 mmol of catalyst. [g]0.0001 mmol of catalyst. [h]In the presence of LiOTF as Lewis acid additive, DBU/LiOTf = 7.5. [i]TON = (mmol of formate)/(mmol of catalyst). [j]Yields calculated from the integration of ^1H NMR signals due to $NaHCO_2$, using DMF as internal standard. [k]As for footnote a, Hg(0) added.

°C (Table 3, entry 13), whereas a TON of 465 was achieved at 25 °C after 21 h at 80 bar (entry 14). On further reduction of the catalyst loading to 0.005 mol %, CO_2 formate was still achieved with a high TON of 10275, albeit in low yield with respect to the base (21%, entry 15). Lowering the catalyst amount further (0.001 mol %) under the same conditions resulted in a lower TON of 5000 (entry 16). We also tested the effect of additives at high substrate to catalyst ratios. Surprisingly, in contrast to what was observed by Hazari et al.,[4e] the use of a LA cocatalyst such as LiOTf negatively affected the performance (entry 17). Colloidal metal catalysis was ruled out by carrying out a Hg poisoning test, which gave results comparable to those observed in the original run (entry 19 vs 5).

Mechanistic Studies. In order to gain insights into the reaction mechanism, the reactivity of complex **2** was investigated in stoichiometric reactions by NMR techniques. Exposure of an EtOH solution of **2** to H_2 (1 bar) in the presence of KO*t*Bu resulted in the quantitative formation of dihydrides **3a**,**b** (cis and trans isomers).[5c,7] The $^{31}P\{^1H\}$ NMR spectrum exhibits two singlets at 187.5 ppm (**3a**) and 189.9 ppm (**3b**), while the ^1H NMR exhibits a triplet at −9.57 ppm for **3a** and a broad resonance at −13.86 ppm for **3b**. When the temperature is lowered to −50 °C, the broad signal starts to split into two separate triplets centered at −8.82 and −17.64 ppm.[7] Using DBU as base, NMR analysis revealed that only 40% of **2** was converted into the Fe(II) dihydrides **3**, even after prolonged standing under an hydrogen atmosphere, suggesting that **2** and **3** are in equilibrium with each other (Scheme 2, step i). This may be explained by the lower pK_a value of $[DBU\text{-}H]^+$ in comparison to that of tBuOH.[8]

Scheme 2. Stepwise Reaction of 2 with H_2 (i) and CO_2 (ii) in the Presence of DBU as Base in EtOH

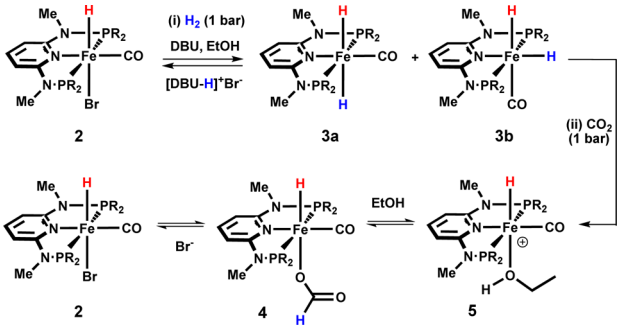

Next, the EtOH/base solution containing in situ formed **3** was stirred under an atmosphere of CO_2 for 30 min. Regardless of the base used, we observed the formation of the hydrido formate complex $[Fe(PNP^{Me}\text{-}iPr)(H)(CO)(\eta^1\text{-}O_2CH)]$ (**4**; Scheme 2, step ii) characterized by a triplet at −24.71 ppm for the hydride and a singlet at 7.96 ppm for the proton of the formate ligand, which both integrate to 1 in the ^1H NMR spectrum (see the Supporting Information).

Under these reaction conditions, **4** is in equilibrium with **2** due to the presence of bromide anions in solution. As a result, a broad signal at 8.65 ppm due to free formate salt appeared in the corresponding ^1H NMR spectrum. In addition, the cationic hydride complex $[Fe(PNP^{Me}\text{-}iPr)(H)(CO)(EtOH)]^+$ (**5**) was present (Scheme 2), exhibiting a ^1H NMR triplet resonance at −25.57 ppm. The $^{31}P\{^1H\}$ NMR chemical shift of **5** is very close to that of formate complex **4**. However, no signal for the free formate counteranion could be found in the ^1H spectrum of **5**. It is worth noting that complex **5** was independently synthesized by treatment of **2** with silver salts in EtOH.[7] In a separate experiment, stirring a mixture of **2** and sodium formate (4 equiv) in EtOH for 1 h also affords a mixture of **2**, **4**, and **5**. In another experiment, this time starting from *isolated* **3**, the reaction with CO_2 in EtOH afforded **5** with minor traces of **4**. Evidently, the formate ligand is easily displaced by an excess of solvent under these conditions.

Single crystals of **4** suitable for X-ray diffraction analysis were obtained by slow diffusion of pentane into a concentrated solution of the complex in THF under an atmosphere of CO_2. The solid-state structure of **4** confirms the geometry proposed on the basis of NMR data. A structural view is depicted in Figure 1 with selected bond distances given in the caption. Complex **4** adopts a distorted-octahedral geometry around the metal center with the formate and hydride ligands trans to each other and in positions cis to the CO ligand. The hydride could be unambiguously located in the difference Fourier maps. The Fe−H distance was refined to 1.46(2) Å.

On the basis of the experimental evidence, a catalytic cycle for CO_2 hydrogenation starting from **2** can be proposed, encompassing formation of dihydrides **3** and CO_2 insertion to give the hydrido formate complex **4** followed by hydrogenolysis and formate elimination giving back **3** in the presence of base. Solvent-assisted formate decoordination in **4** may occur to leave a highly reactive, unobserved pentacoordinate cationic Fe(II) hydrido carbonyl species, which can be stabilized by EtOH coordination to give **5**, observed by NMR (Scheme 3).

DOI: 10.1021/acscatal.6b00416
ACS Catal. XXXX, XXX, XXX−XXX

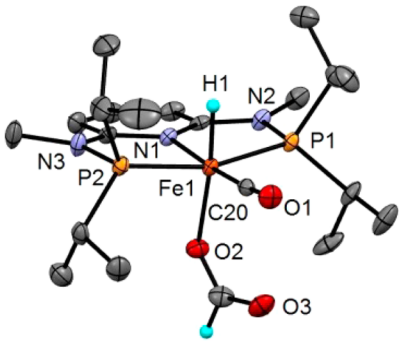

Figure 1. Structural view of **4** showing 50% thermal ellipsoids (most H atoms and a second independent complex omitted for clarity). Selected bond lengths (Å) and angles (deg): Fe1−P1 2.1765(7), Fe1−P2 2.1789(7), Fe1−N1 2.004(2), Fe1−C20 1.737(2), Fe1−O2 2.032(2), Fe1−H1 1.46(2); P1−Fe1−P2 162.57(2), N1−Fe1−C20 175.58(8).

Scheme 3. Proposed Catalytic Cycle for CO_2 Hydrogenation with 3a

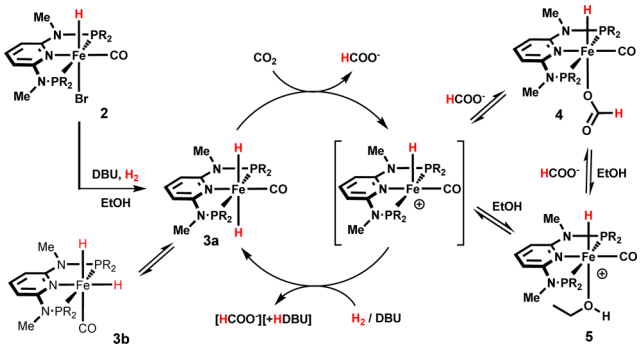

Further mechanistic details on the CO_2 hydrogenation mechanism were obtained by DFT calculations using **3a** as the initial active species. The free energy profile is shown in Scheme 4. Computational details are presented as Supporting Information. The model used in the calculations included one explicit water molecule that provides H-bond stabilization of the intermediates. The highlights of the calculated mechanism are presented in Scheme 4 with relevant intermediates and the corresponding free energy values.[9]

Scheme 4. Free Energy Profile Calculated (DFT) for the Hydrogenation of CO_2 Catalyzed by 3a (Denoted as A)[a]

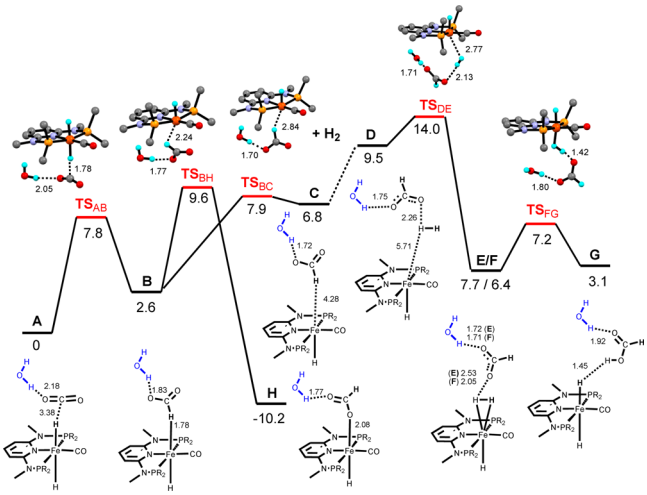

[a]The free energy values (kcal/mol) are referenced to the initial reactants, and relevant distances (Å) are indicated.

In the first step of the calculated mechanism, from **A** to **B**, the hydride attack from complex **3a** to a CO_2 molecule results in a H-bonded formate complex. This is a facile process with a barrier of 7.8 kcal/mol. In the resulting intermediate (**B**) the formate ion is stabilized by a H-bond with the water molecule. From **B**, formate can coordinate the metal, giving complex **4** (**H** in Scheme 4), where the formate ligand is bonded through the O atom. This intermediate represents the potential well of the mechanism; thus, it may be viewed as the catalyst resting state. Alternatively, the formate ion dissociates from the metal in **B** to give **C**, opening one coordination position that is occupied by a molecule of H_2 in the following step. Both processes are competitive with barriers within 2 kcal/mol. The reaction pathway proceeds with H_2 addition to **C**, yielding the dihydrogen complex **F**. This process has an energy barrier of 14 kcal/mol, corresponding to the highest barrier of the entire mechanism. In the final step, the formate ion is protonated by **F**, regenerating the initial complex **3a** and producing formic acid. Given the excess of base present in the reaction medium under experimental conditions, the acid formed will then be deprotonated in an acid−base reaction that provides the final driving force for the entire process. Importantly, the free formate ion (the reaction product under the experimental conditions) is stabilized by a H bond with the nearby water molecule in intermediates **E**/**F**.[9] This facilitates the opening of the coordination position that will be used by H_2 in the following step of the mechanism, justifying the need for a protic solvent in the catalytic reaction. A similar reaction mechanism was recently proposed for the selective hydrogenation of aldehydes in EtOH with **3** as catalyst[7] and by other authors on related systems.[10]

CONCLUSIONS

In conclusion, selected Fe(II) pincer-type complexes of 2,6-diaminopyridylbis(diisopropylphosphine) gave high activities as catalysts for CO_2 and $NaHCO_3$ reduction to formate under very mild to moderate conditions, even at room temperature. Mechanistic details were obtained by NMR techniques, highlighting the role of dihydride and hydrido formate complexes. DFT calculations indicate an outer-sphere mechanism with a hydrido formate complex as the catalyst resting state and suggest that the overall reaction is pushed forward by the acid−base reaction between the product (formic acid) and the excess base present in solution. Protic solvents promote catalysis by stabilizing the reaction intermediates and assisting formate elimination from the coordination sphere of the metal.

ASSOCIATED CONTENT

Supporting Information

The Supporting Information is available free of charge on the ACS Publications website at DOI: 10.1021/acscatal.6b00416.

General materials and methods, synthetic procedures, NMR experiments and spectra, Cartesian coordinates of the computed structures, crystallographic data for the X-ray structure of **4**, and additional catalytic data (PDF)
Crystallographic data for the X-ray structure of **4** (CIF)

DOI: 10.1021/acscatal.6b00416
ACS Catal. XXXX, XXX, XXX−XXX

AUTHOR INFORMATION

Corresponding Authors

*E-mail for K.K.: karl.kirchner@tuwien.ac.at.

*E-mail for L.G.: l.gonsalvi@iccom.cnr.it.

Notes

The authors declare no competing financial interest.

ACKNOWLEDGMENTS

Financial contributions by the CNR and ECRF through projects EFOR and HYDROLAB-2.0, respectively, are gratefully acknowledged. This work was also supported by COST Action CM1205 CARISMA (Catalytic Routines for Small Molecule Activation). L.F.V. acknowledgesthe Fundação para a Ciência e Tecnologia, grant UID/QUI/00100/2013. N.G. and K.K. gratefully acknowledge financial support by the Austrian Science Fund (FWF) (Project No. P24583-N28).

REFERENCES

(1) (a) Joó, F. *ChemSusChem* **2008**, *1*, 805−808. (b) Enthaler, S.; von Langermann, J.; Schmidt, T. *Energy Environ. Sci.* **2010**, *3*, 1207−1217. (c) Loges, B.; Boddien, A.; Gärtner, F.; Junge, H.; Beller, M. *Top. Catal.* **2010**, *53*, 902−914.

(2) (a) Papp, G.; Csorba, J.; Laurenczy, G.; Joó, F. *Angew. Chem., Int. Ed.* **2011**, *50*, 10433−10435. (b) Boddien, A.; Gärtner, F.; Federsel, C.; Sponholz, P.; Mellmann, D.; Jackstell, R.; Junge, H.; Beller, M. *Angew. Chem., Int. Ed.* **2011**, *50*, 6411−6414.

(3) Wang, W.-H.; Himeda, Y.; Muckerman, J. T.; Manbeck, G. F.; Fujita, E. *Chem. Rev.* **2015**, *115*, 12936−12973.

(4) (a) Federsel, C.; Boddien, A.; Jackstell, R.; Jennerjahn, R.; Dyson, P. J.; Scopelliti, R.; Laurenczy, G.; Beller, M. *Angew. Chem., Int. Ed.* **2010**, *49*, 9777−9780. (b) Ziebart, C.; Federsel, C.; Anbarasan, P.; Jackstell, R.; Baumann, R.; Spannenberg, W. A.; Beller, M. *J. Am. Chem. Soc.* **2012**, *134*, 20701−20704. (c) Bertini, F.; Mellone, I.; Ienco, A.; Peruzzini, M.; Gonsalvi, L. *ACS Catal.* **2015**, *5*, 1254−1265. (d) Langer, R.; Diskin-Posner, Y.; Leitus, G.; Shimon, L. J. W.; Ben-David, Y.; Milstein, D. *Angew. Chem., Int. Ed.* **2011**, *50*, 9948−9952. (e) Zhang, Y.; MacIntosh, A. D.; Wong, J. L.; Bielinski, E. A.; Williard, P. G.; Mercado, B. Q.; Hazari, N.; Bernskoetter, W. *Chem. Sci.* **2015**, *6*, 4291−4299. (f) Rivada-Wheelaghan, O.; Dauth, A.; Leitus, G.; Diskin-Posner, Y.; Milstein, D. *Inorg. Chem.* **2015**, *54*, 4526−4538.

(5) (a) Bichler, B.; Glatz, M.; Stöger, B.; Mereiter, K.; Veiros, L. F.; Kirchner, K. *Dalton Trans* **2014**, *43*, 14517−15419. (b) de Aguiar, S. R. M. M.; Öztopcu, Ö.; Stöger, B.; Mereiter, K.; Veiros, L. F.; Pittenauer, E.; Allmaier, G.; Kirchner, K. *Dalton Trans* **2014**, *43*, 14669−14679. (c) Gorgas, N.; Stöger, B.; Veiros, L. F.; Pittenauer, E.; Allmaier, G.; Kirchner, K. *Organometallics* **2014**, *33*, 6905−6914. (d) Bichler, B.; Holzhacker, C.; Stöger, B.; Puchberger, M.; Veiros, L. F.; Kirchner, K. *Organometallics* **2013**, *32*, 4114−4121. (e) Benito-Garagorri, D.; Becker, E.; Wiedermann, J.; Lackner, W.; Pollak, M.; Mereiter, K.; Kisala, J.; Kirchner, K. *Organometallics* **2006**, *25*, 1900−1913. (f) Benito-Garagorri, D.; Wiedermann, J.; Pollak, M.; Mereiter, K.; Kirchner, K. *Organometallics* **2007**, *26*, 217−222. (g) Benito-Garagorri, D.; Puchberger, M.; Mereiter, K.; Kirchner, K. *Angew. Chem., Int. Ed.* **2008**, *47*, 9142−9145.

(6) Over-quantitative yields of formate have been reported with DBU as base; see: Hsu, S.-F.; Rommel, S.; Eversfield, P.; Muller, K.; Klemm, E.; Thiel, W. R.; Plietker, B. *Angew. Chem., Int. Ed.* **2014**, *53*, 7074−7078. See also ref 4e and references cited therein.

(7) Gorgas, N.; Stöger, B.; Veiros, L. F.; Kirchner, K. *ACS Catal.* **2016**, *6*, 2664−2672.

(8) The pK_a for DBU is ca. 11.5−11.9; see: Kaupmees, K.; Trummal, A.; Leito, I. *Croat. Chem. Acta* **2014**, *87*, 385−395. The pK_a for *t*BuOH in water is 17.

(9) Free energy values were obtained at the B3LYP/VDZP level using the Gaussian 09 package. All calculations included solvent effects (THF) using the PCM/SMD model. A full account of the computational details and a complete list of references are provided as Supporting Information.

(10) Yang, X. *Inorg. Chem.* **2011**, *50*, 12836−12843.

DOI: 10.1021/acscatal.6b00416
ACS Catal. XXXX, XXX, XXX−XXX